PHYSICAL REVIEW B **91**, 020201(R) (2015)

High-Q optical cavities in hyperuniform disordered materials

Timothy Amoah and Marian Florescu*

Advanced Technology Institute and Department of Physics, University of Surrey, Guildford GU2 7XH, United Kingdom

(Received 15 September 2014; revised manuscript received 18 December 2014; published 20 January 2015)

We introduce designs for high-Q photonic cavities in slab architectures in hyperuniform disordered solids displaying isotropic band gaps. Despite their disordered character, hyperuniform disordered structures have the ability to tightly confine the transverse electric-polarized radiation in slab configurations that are readily fabricable. The architectures are based on carefully designed local modifications of otherwise unperturbed hyperuniform dielectric structures. We identify a wide range of confined cavity modes, which can be classified according to their approximate symmetry (monopole, dipole, quadrupole, etc.) of the confined electromagnetic wave pattern. We demonstrate that quality factors $Q > 10^9$ can be achieved for purely two-dimensional structures, and that for three-dimensional finite-height photonic slabs, quality factors $Q > 20\,000$ can be maintained.

DOI: 10.1103/PhysRevB.91.020201 PACS number(s): 41.20.Jb, 42.70.Qs, 78.66.Vs, 85.60.Jb

A special class of disordered photonic heterostructures has recently been shown to display large isotropic band gaps comparable in width to band gaps found in photonic crystals [1–3]. The large band gaps found in these structures are facilitated by the hyperuniform geometrical properties of the underlying point-pattern template upon which the structures are built. The statistical isotropy of the photonic properties of these materials is highly relevant for a series of novel photonic functionalities including arbitrary angle emission or absorption and free-form waveguiding [3,4].

A point pattern in real space is hyperuniform if for large R the number variance $\sigma(R)^2$ within a spherical sampling window of radius R (in d dimensions) grows more slowly than the window volume, i.e., more slowly than R^d. In Fourier space, hyperuniformity means that the structure factor $S(\mathbf{k})$ approaches zero as $|\mathbf{k}| \to 0$ [5,6]. The lack of periodicity in these hyperuniform disordered (HUD) solids demonstrates that Bragg scattering is not a prerequisite for photonic band gaps (PBGs) and that interactions between local resonances and multiple scattering are sufficient, provided that the disorder is constrained to be hyperuniform [1].

The concept of optical cavities in HUD photonic materials was recently introduced in Ref. [7]. The structure analyzed was obtained by placing dielectric rods at each point of a hyperuniform point pattern. The radius of one selected rod was varied to achieve localization of the transverse magnetic (TM)-polarized electromagnetic field at that point. The study was based purely on two-dimensional (2D) structures, and vertical confinement, the primary loss pathway in real slab structures, was not discussed. The question of how to achieve index guiding and the essential vertical confinement in disordered photonic slab structures, a prerequisite of realizing cavities with high-quality factors, which can be fabricated using conventional techniques and are fully compatible with existing photonic-circuit layouts, was seen as a potential roadblock in the HUD photonic materials field.

In this Rapid Communication we introduce finite-height network structures for localizing transverse electric (TE)-polarized radiation and analyze the vertical confinement issue. The structures analyzed are composed of polygonal cells of dielectric walls. The protocol for generating these structures described in Refs. [1,8] consists of Delaunay triangulating over a hyperuniform point pattern and connecting the center of mass of the Delaunay triangles to form cells that contain one original point each. The walls of the resulting network are then given a finite thickness. The structure presents well-defined short-range order and long-range statistical isotropy. Recently, these designs have been fabricated on the microwave scale and successfully tested [9].

We begin our analysis with the study of purely 2D structures. A length scale $a = L/\sqrt{N}$ is defined, such that an N-point hyperuniform pattern in a square box of side length L has density of $1/a^2$. The structure parameters are set to $\epsilon = 11.56$ for the dielectric constant and the wall width is set to $w = 0.2a$. For our study, we employ a point pattern containing $N = 500$, with a hyperuniformity order parameter $\chi = 0.5$ [10] [here, χ is defined as the ratio between the number of $\mathbf{k}$ vectors for which the structure factor $S(k)$ is constrained to vanish and the total number of $\mathbf{k}$ vectors]. We calculate the photonic band structure using the eigenmode expansion software MPB for a $\sqrt{N}a \times \sqrt{N}a$ sample and identify the PBG edges. We then run a sweep for varying wall thickness (w) and find the largest PBG with $\Delta\omega/\omega_C = 30.7\%$ for $w = 0.23a$, where $\Delta\omega$ is the band gap width and ω_C is the band gap center frequency. Similar to other conventional disordered structures, unperturbed HUD structures display defect modes. These Anderson-like localized modes, shown in Fig. 1, occur naturally at the PBG edges and extend over over network domains comprising five to ten cells. Sparsely occurring are accidental localized modes extending on one to three network cells which are promoted into the PBG due to the local topology, but we are not exploring these here [11].

In an otherwise unperturbed structure, it is possible to create an intentional localized state of the electromagnetic field by reducing or enhancing the dielectric constant at a certain point in the structure. For a triangular lattice of holes it is common practice to fill a single hole to make a cavity which is often labeled a 1 cavity. In analogy to this, we fill a single cell and also label it H1. Due to the presence of the defect, four localized cavity modes are created within the PBG at specific frequencies. The mode profiles are shown in Fig. 2. Two of the modes are dipolelike and the other two modes are quadrupolelike. We denote the lower frequency

*m.florescu@surrey.ac.uk

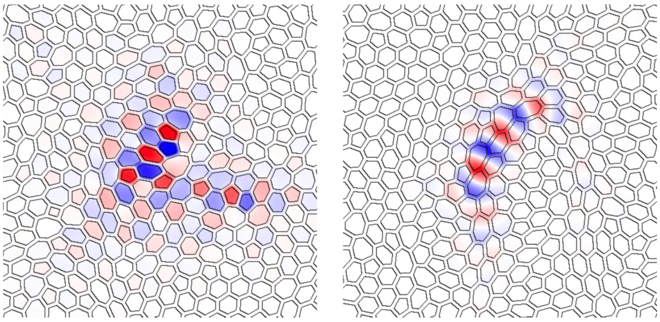

FIG. 1. (Color online) Magnetic field distributions of two Anderson-like localized modes, below the lower (left) and above the upper (right) PBG edge, respectively.

dipole mode D_1 and the higher frequency dipole mode D_2. The cavity has an approximately hexagonal shape, as such we can describe the modes according to the approximate symmetries associated with a hexagonal unit cell in a triangular lattice. For the D_1 mode the nodal axis of the H_z component of the electromagnetic field lies approximately along the faux K direction and the mode is propagation confined along the faux M direction. For the D_2 mode the nodal axis of the H_z component of the electromagnetic field lies approximately along the faux M direction and the mode is propagation confined along the faux K direction. The magnetic field distribution of the cavity modes shown in Fig. 2 suggests very good in-plane confinement and calculations of the quality factors (using the finite difference time domain software MEEP [12]) confirms that the quality factor for all modes higher than 10^9.

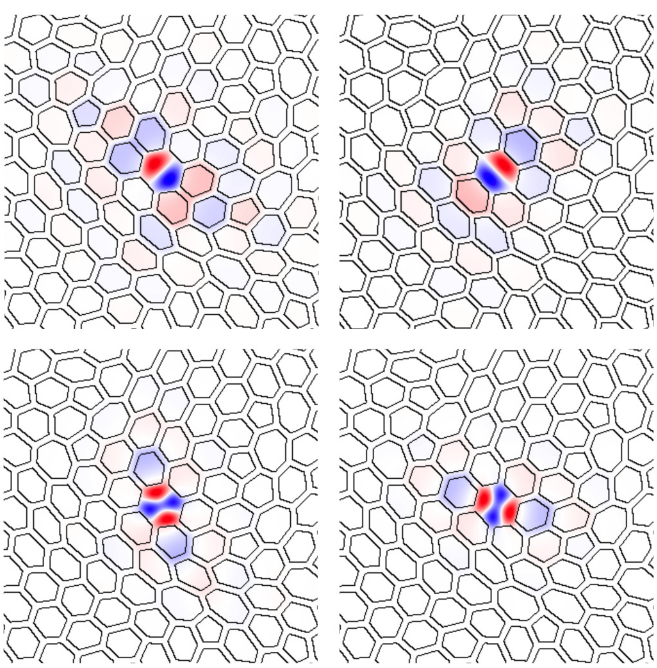

FIG. 2. (Color online) Magnetic field distribution for the four defect modes in the unmodified H1 cavity in a structure of wall thickness $w = 0.2a$. The modes are labeled D_1, D_2, Q_1, Q_2 (shown from left to right in the figure).

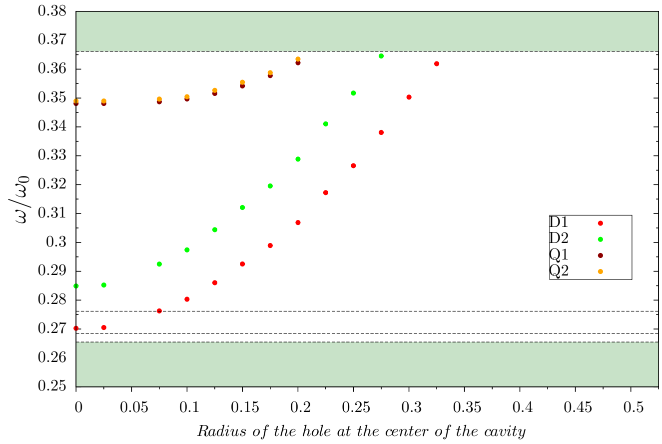

FIG. 3. (Color online) Frequencies of the cavity modes in the band gap obtained for different radii of a hole placed at the center of the cavity.

To study the frequency behavior of the cavity modes as a function of dielectric filling of the defect cell, we place a circular air hole at the center of the unmodified H1 cavity, vary its radius from $r = 0$ to $r = 0.535a$, and monitor the evolution of the cavity mode frequencies. The general trend is that the frequency of the cavity modes increases with the radius of the hole. In other words, the mode frequency is lowered by the inclusion of more dielectric, which demonstrates that the cavity originates from modes above the upper band edge of the unperturbed structure.

We now turn our investigation towards the photonic-slab architectures where we can no longer neglect the vertical extent of the structure. This is similar to the concept of photonic-crystal slabs [13,14], which has proven to be a promising platform for photonic microcircuitry. In photonic slabs, while there exists no true PBG, the existence of "pseudoband gaps" enables low-loss waveguiding and high-Q cavities [15]. The "pseudoband gap" is associated with an effective gap in the in-plane band structure for which modes below the light cone cannot couple to the continuum of states outside the slab. The projected band structure method only works well when only a single in-plane unit cell is considered. For supercell calculations, the spectral regions with no effective band gap will be translated onto the region of the effective band gap, through the "supercell folding" effect. With no straightforward method to circumvent this we will resort to making the assumptions that a pseudoband gap does exist for the photonic slab, and that if a cavity mode of specific form were to lie within

TABLE I. The mode frequencies in the 2D and 3D case and Q factor for the modified H1 cavity with a $0.2a$ inner hole.

Mode	ω/ω_0 in plane	ω/ω_0 slab	Q factor
D_1	0.22482	0.26722	7976
D_2	0.23775	0.28003	8672
Q	0.24546	0.28811	2561
H	0.25133	0.29385	4845
O	0.25916	0.29973	3230

RAPID COMMUNICATIONS

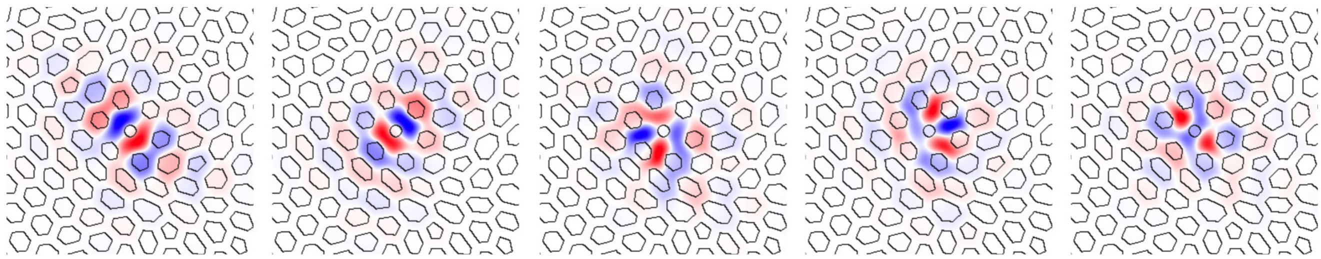

FIG. 4. (Color online) Magnetic field distribution for the five cavity modes in the enlarged H1 cavity with center hole $r = 0.2a$ in a structure of wall thickness $w = 0.4a$. The modes are labeled D_1, D_2, Q, H, O, left to right.

the band gap when calculated in 2D, it would also lie within the pseudoband gap for the photonic slab. Consequently, the frequencies in Fig. 3 are the in-plane frequencies, not the slab frequencies.

For photonic slabs, it is not generally true that the best optical confinement is achieved for the largest in-plane PBG. For a large enough sample the main losses occur in the vertical direction, and to prevent them one needs to rely on index confinement. As such, the thicker walls translate into a higher effective index for the slab and hence better vertical confinement. For our structures, we use a structure height of $h = 0.7a$, and double the wall width to $w = 0.4a$ to improve confinement. For an unmodified H1 cavity the expected quality factor is typically rather moderate even for a conventional photonic crystal, $Q < 500$ [16]. We calculate $Q = 210$ for the D_1 and $Q = 190$ for the D_2 mode. These values can be considerably increased by placing an inner hole at the center of the cavity (see Table I).

A conventional method for achieving optimal designs is to reduce adjacent holes slightly in size and shift them outwards along the lattice directions. In the disordered case there are no lattice directions, and we instead shift the shrunken cells along the vector given by the center of mass of the cavity to the center of mass of the neighboring cell. The cells are shrunken to 52% of the size of a cell with infinitesimal walls and are shifted by 8% of the length of the vector outwards. For a modified cell cavity we find five cavity modes lying in the band gap (see Figs. 4 and 5). The lowest frequency mode is again the D_1 mode, followed by the D_2 mode. An isocontour plot of the electric field intensity distribution of the D_1 mode is shown in Fig. 6, displaying in-plane PBG-mediated confinement and vertical refractive index confinement. As expected, the two dipole modes now have lower frequencies due to the addition of dielectric material. The higher frequency modes are a quadrupolelike mode (Q) and a hexapolelike mode (H). We note that (due to disorder) the symmetry separation of the two modes is not entirely complete. Lastly, there is the highest frequency mode, which is rather difficult to define. The H_z field is symmetric with respect to the faux K direction; therefore the mode is an odd mode. We can identify four nodes lying "within" the cavity, so it can either be considered a second quadrupole mode or an octapole mode. Due to its higher frequency, we label it as an octapolelike mode (O).

Figure 7 shows the spatially Fourier transformed in-plane fields of the D_1 and D_2 cavity modes for both the unmodified and modified (extra central hole) cavity. The corresponding light circles are indicated by the white dots. Only the Fourier components with $k < \omega c$ can radiate into the far field, and hence the more Fourier components that are within the light circle, the greater the radiative loses in the vertical direction. Clearly, the modified-cavity design in Fig. 7 displays a considerably smaller number of radiative components.

Finally, we consider optimal cavity designs for the O mode. For a neighbor cell size of 44% at the same center of mass shift of 8%, we find a very-high-quality factor of $Q = 20\,148$,

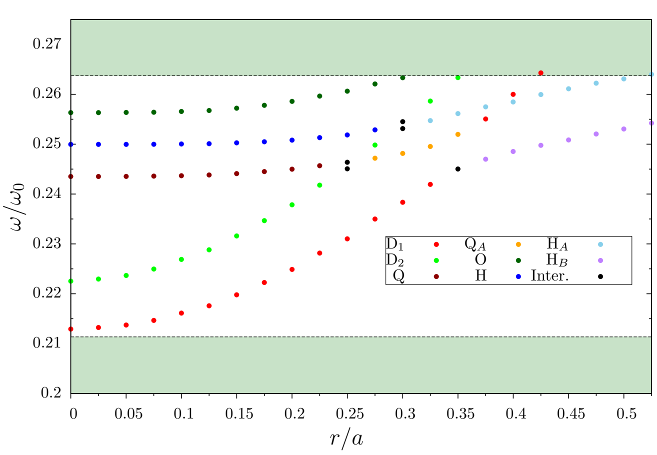

FIG. 5. (Color online) Frequencies of the cavity modes in the band gap obtained for different radii of a hole placed at the center of the cavity. Modes are labeled according to their number of pole lobes and their approximate symmetry. Different colors are used for modes with the same number of lobes and same approximate symmetry, but have distinct field patterns. Crossover intermediate modes are colored black.

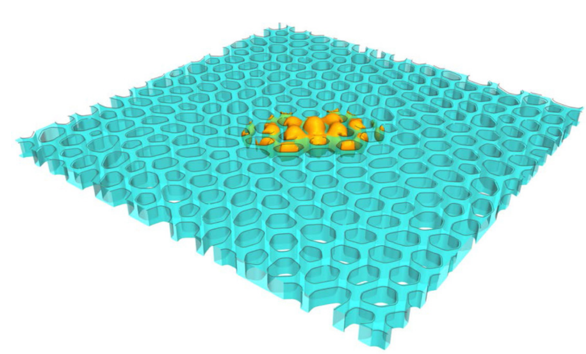

FIG. 6. (Color online) Intensity distribution (yellow) of a confined cavity mode in a hyperuniform disordered honeycomb photonic slab (blue).

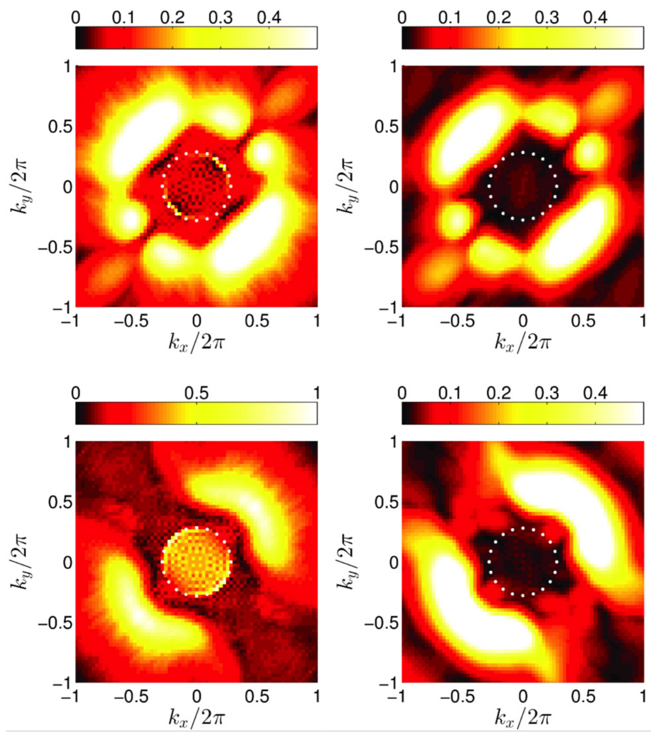

FIG. 7. (Color online) Spectrum of the Fourier components of the electric field distribution for the D_1 mode before (top left) and after modification (top right) and D_2 mode before (bottom left) and after modification (bottom right). Logarithmic color scale.

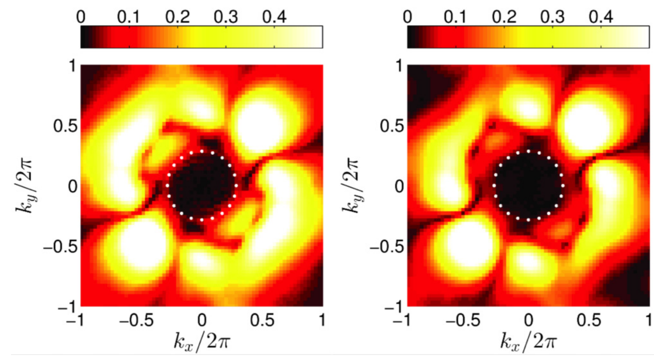

FIG. 8. (Color online) Spectrum of the Fourier components of the electric field distribution for a modified cavity with neighbor cell size of 52% (left) and 44% (right), both shifted by 8%. Logarithmic color scale.

which is significantly larger than $Q = 3230$ obtained at 52% neighbor cell size. Figure 8 shows the Fourier spectrum in each respective case. As before, the Fourier components in the light circle are reduced for the higher-quality modification. However, the most significant factor is the change in frequency from 0.299 73 to 0.287 02. As a result of this displacement, the mode is now localized in the spectral domain where the radiative losses are minimized.

In summary, we have introduced architectures for the design of optical cavities in a hyperuniform disordered material. We have demonstrated that H1-type cavity defects can support localized modes with a variety of symmetries and multiple frequencies. The ability to localize modes of different symmetry and frequency in the same physical cavity and to guide light through modes with different localization properties can have a great impact on all-optical switching [17], implementations of linear-optical quantum information processors [18], and single-photon sources [19,20].

The physical nature of the localized modes in HUD materials is very different from that of cavity modes in structures with long-range order (photonic crystals [16] and quasicrystals [21]). The very nature of the PBG is quite different: In long-range ordered media Bragg scattering plays an essential role in the formation of the PBG, whereas for HUD structures there is no Bragg scattering and the PBG formation relies solely on localized scattering resonances [1]. The removal of the constraints associated with long-range order has a major impact on the properties of the localized modes: A fixed cavity (defined as a geometrical or topological defect) in an HUD surround supports a large variety of localized modes with (approximate) symmetries or no obvious symmetry at all. Moreover, as we demonstrate here, all these modes can be optimized to provide tight confinement on par with that provided by ordered media. Vertical confinement in disordered materials is an essential requirement for fabrication using traditional complementary metal-oxide semiconductor (CMOS)-compatible techniques and integration in conventional photonic-circuit layouts. On a fundamental level, one may presume that disorder would facilitate significant out-of-plane scattering as compared to periodic structures. Here, we have demonstrated that for cavities built on hyperuniform platforms, by adequately adjusting the structure parameters and cavity design, it is possible to achieve very tight optical confinement.

Our successful demonstration of a high-Q cavity for TE-polarized radiation is encouraging for future investigations of TE waveguides in disordered photonic slabs. These would be promising candidates for achieving highly flexible and robust platforms for integrated optical microcircuitry.

ACKNOWLEDGMENTS

This work was supported by the EPSRC (United Kingdom) DTG Grant No. KD5050. M.F. also acknowledges support from EPSRC (United Kingdom) Strategic Equipment Grant No. EP/M008576/1 and the University of Surrey (United Kingdom) FRSF, Santander, and IAA awards.

[1] M. Florescu, S. Torquato, and P. J. Steinhardt, Proc. Natl. Acad. Sci. USA **106**, 20658 (2009).

[2] W. Man, M. Florescu, E. P. Williamson, Y. He, S. R. Hashemizad, B. Y. C. Leung, D. R. Liner, S. Torquato, P. Chaikin, and P. Steinhardt, Proc. Natl. Acad. Sci. USA **110**, 15886 (2013).

[3] W. N. Man, M. Florescu, K. Matsuyama, P. Yadak, G. Nahal, S. Hashemizad, E. Williamson, P. Steinhardt, S. Torquato, and P. Chaikin, Opt. Express **21**, 19972 (2013).

[4] K. Vynck, M. Burresi, F. Riboli, and D. S. Wiersma, Nat. Mater. **11**, 1017 (2012).

[5] S. Torquato and F. H. Stillinger, Phys. Rev. E **68**, 041113 (2003).

[6] C. E. Zachary and S. Torquato, J. Stat. Mech.: Theor. Exp. (2009) P12015.

[7] M. Florescu, S. Torquato, and P. J. Steinhardt, Phys. Rev. B **87**, 165116 (2013).

[8] M. Florescu, P. J. Steinhardt, and S. Torquato, Phys. Rev. B **80**, 155112 (2009).

[9] M. Florescu *et al.*, Proc. SPIE **9162**, 91620G (2014).

[10] R. D. Batten, F. H. Stillinger, and S. Torquato, J. Appl. Phys. **104**, 033504 (2008).

[11] M. Florescu, S. Torquato, and P. J. Steinhardt, Appl. Phys. Lett. **97**, 201103 (2010).

[12] A. Oskooi, D. Roundy, M. Ibanescu, P. Bermel, J. D. Joannopoulos, and S. G. Johnson, Comput. Phys. Commun. **181**, 687702 (2010).

[13] Y. Akahane, T. Asano, B. Song, and S. Noda, Nature (London) **425**, 944 (2003).

[14] J. D. Joannopoulos, S. G. Johnson, J. N. Winn, and R. D. Meade, *Photonic Crystals: Molding the Flow of Light*, 2nd ed. (Princeton University Press, Princeton, NJ, 2008).

[15] S. G. Johnson, S. Fan, P. Villeneuve, J. Joannopolous, and L. Kolodziejski, Phys. Rev. B **60**, 5751 (1999).

[16] A. Tandaechanurat, S. Iwamoto, M. Nomura, N. Kumagai, and Y. Arakawa, Opt. Express **16**, 448 (2008).

[17] M. Florescu and S. John, Phys. Rev. A **69**, 053810 (2004).

[18] F. M. Spedalieri, H. Lee, M. Florescu, K. T. Kapale, U. Yurtsever, and J. P. Dowling, Opt. Commun. **254**, 374 (2005).

[19] M. Florescu, S. Scheel, H. Hffner, H. Lee, D. V. Strekalov, P. L. Knight, and J. P. Dowling, Europhys. Lett. **69**, 945 (2005).

[20] S. Scheel, M. Florescu, H. Haffner, H. Lee, D. V. Strekalov, P. L. Knight, and J. P. Dowling, J. Mod. Opt. **54**, 409 (2007).

[21] S. M. Thon, W. T. M. Irvine, D. Kleckner, and D. Bouwmeester, Phys. Rev. Lett. **104**, 243901 (2010).